Phase-Synchronization, Energy Cascade, and Intermittency in Solar-Wind Turbulence

S. Perri, V. Carbone, A. Vecchio, R. Bruno, H. Korth, T. H. Zurbuchen, and L. Sorriso-Valvo

Phys. Rev. Lett. **109**, 245004 — Published 11 December 2012

DOI: 10.1103/PhysRevLett.109.245004

Phase-synchronization, energy cascade and intermittency in the solar wind turbulence

S. Perri[1], V. Carbone[1,2], A. Vecchio[1], R. Bruno[3],
H. Korth[4], T.H. Zurbuchen[5], and L. Sorriso-Valvo[2,6]

[1] *Dipartimento di Fisica,*
Università della Calabria,
87036 Rende (CS), Italy;

[2] *IPCF-CNR, Ponte P. Bucci,*
Cubo 31C, 87036 Rende (CS), Italy;

[3] *IFSI-INAF, Via Fosso del Cavaliere,*
I-00133 Roma, Italy;

[4] *The Johns Hopkins University Applied Physics Laboratory,*
Laurel, MD 20723, USA;

[5] *Department of Atmospheric,*
Oceanic and Space Sciences,
University of Michigan,
Ann Arbor, MI 48109, USA.

[6] *Space Sciences Laboratory - University*
of California at Berkeley 7 Gauss way,
Berkeley, 94720 CA, USA.

Abstract

The energy cascade in solar wind magnetic turbulence is investigated using MESSENGER data in the inner heliosphere. Decomposition of magnetic field time series in intrinsic functions, each characterized by a typical timescale, reveals phase re-organization. This allows for the identification of structures of all sizes generated by the nonlinear turbulent cascade, covering both the inertial and the dispersive ranges of the turbulent magnetic power spectrum. We find that the correlation (or anticorrelation) of phases occurs between pairs of neighboring timescales, whenever localized peaks of magnetic energy are present at both scales, consistent with the local character of the energy transfer process.

PACS numbers: 94.05.-a; 52.35.Ra; 94.05.Lk

The mechanism of turbulent energy cascade in fluids [1] and in magnetized fluid flows [2] is still poorly understood. This process involves many coupled degrees of freedom and exhibit universal and nontrivial scaling behavior [1, 3]. According to Richardson's phenomenology [4], the turbulent energy cascades from eddies at a scale ℓ to eddies at smaller (but comparable) scales $\ell' < \ell$ [5]. Experiments suggest that the energy transfer is not steady but intermittent, exhibiting strong bursts of activity in between relatively quiescent periods [1, 6]. Non-homogeneity of the energy transfer is described, for example, by the multifractal model [7], which takes into account the concentration of energy in "active eddies" [1] while cascading towards smaller scales. According to the multifractal model, the energy cascade spontaneously generates isolated bursts of fluctuations on all spatial scales [8, 9].

In order to identify turbulent structures in experimental data, intermittent bursts of turbulent activity have often been related to the presence of convected coherent structures such as ribbons, tubes or sheets of vorticity, as well as localized current sheets in magnetized fluids [2, 9, 10]. Such structures of a given scale are generally considered as isolated features embedded in a random Gaussian background [11]. Arbitrary threshold methods are commonly used to detect isolated structures, which should be characterized by phase correlations in the field [2]. In the solar wind, those isolated structures can develop in the process of turbulent energy cascade down to smaller scales, although the existence of structures of solar origin, generated at relatively large scale and not arising from a cascade process, cannot be ruled out. On the other hand, the presence of the energy cascade is associated with the scaling of the third-order structure function (Yaglom's law) [1, 12], which has no intermittent corrections. Yaglom's law suggests that fluctuations are generated *on all scales* by the cascade process, and that fluctuations on different scales should be somehow connected, for example through phase synchronization.

The solar wind represents the largest laboratory for direct investigation of plasma turbulence [2]. The degree of complexity is enhanced by the existence of many characteristic scales, related to different physical processes. This means that the mechanism of energy transfer among scales depends on the scale itself. Indeed, within the Magnetohydrodynamic (MHD) range, solar wind turbulence exhibits a Kolmogorov-like power law energy spectrum in the wave vector k space, $\sim k^{-5/3}$ [2], while in the dissipative (or dispersive) range, the spectrum steepens beyond the proton scales ($\sim k^{-\alpha}$, with $\alpha \in [2, 4]$) [13, 14]. In this letter we show the first evidence of phase synchronization between structures on different scales

in solar wind, generated by the turbulent cascade of magnetic energy.

Our analysis of solar wind data is based on the combined use of the Empirical Mode Decomposition (EMD) [15] and of wavelet analysis [16]. The former provides a decomposition of solar wind turbulent fields in a limited number of modes (including information on the phase), while the latter enables the detection of intermittent structures and energy transfer in the flow. EMD has been originally developed to process nonstationary and nonlinear data [15], such as experimental turbulence records [17]. However, it further has been applied succesfully to a variety of physical systems [18–21]. A turbulent field $B(t)$ is decomposed into a finite number n of intrinsic mode functions (IMFs), as

$$B(t) = \sum_{j=1}^{n} \mathrm{IMF}_j(t) + r_n(t)\,. \tag{1}$$

IMFs can be written as $\mathrm{IMF}_j(t) = A_j(t)\cos\Phi_j(t)$, where $A_j(t)$ and $\Phi_j(t)$ represent the amplitude and the phase of the j-th mode, respectively; thus they are zero-mean oscillating functions, experiencing both amplitude and frequency modulations. Each IMF is characterized by a time dependent $\omega_j(t)$, and a typical time scale can be obtained by averaging over the whole time interval. Therefore, at variance with the classical Fourier decomposition, the characteristic timescale τ_j for IMFs is an average timescale. The residue $r_n(t)$ in Equation (1) describes the mean trend. EMD is local, complete and orthogonal. It therefore allows the reconstruction of the signal through partial sums in Equation (1). When applied to real data, the dynamic behavior of the system is represented by a limited number of modes n.

Wavelet analysis, on the other hand, provides useful information on the frequency and in time energy distribution of a time series. In order to identify intermittent bursts of energy at different time scales, the Local Intermittency Measure (LIM) [16, 22] has been applied to turbulent data. LIM is defined as

$$\mathrm{LIM}_{\tau,t} = \frac{|\tilde{b}_{\tau,t}|^2}{\langle|\tilde{b}_{\tau,t}|^2\rangle_t}, \tag{2}$$

where $\tilde{b}_{\tau,t}$ is the wavelet coefficient of a component of the magnetic field vector at time t and timescale τ. Brackets $\langle\cdot\rangle$ in equation (2) indicate time average. For each frequency $1/\tau$, the condition $\mathrm{LIM} > 1$ identifies portions of the sample whose power (estimated as the squared wavelet coefficient) is above the average, within the time series. Therefore, such portions

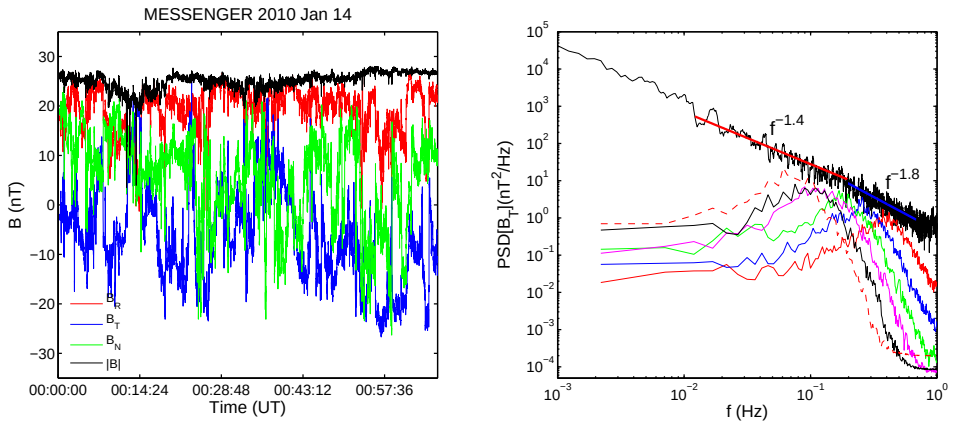

FIG. 1. Time evolution of the magnetic field components in the RTN reference frame and of the magnetic field magnitude (left panel). The power spectrum of the B_T component along with the power law best fits both in the inertial (thick red line) and in the high frequency range (thick blue line) (right panel). In the right panel the spectra of IMFs above and below the spectral break frequency are also displayed (thin red, thin blue, green, magenta, thin black, and red dashed lines). For example, the thin red curve has a peak around 0.4 Hz, which is the average frequency of the highest frequency mode computed.

may represent intermittent structures, where magnetic energy accumulates [23] during the nonlinear energy cascade.

In this work we proceed as follows: after applying EMD to each solar wind magnetic field vector component we investigate the phase difference of IMFs at two neighboring timescales (τ_i, τ_j). Then, we look for the simultaneous presence of intermittent structures at the same pair of neighboring timescales, as detected by LIM, being an indication of energy transfer between such scales.

For our study, we analyze solar wind magnetic field measurements in the inner Heliosphere, using 2 Hz sampled data from the MAG experiment onboard the MESSENGER spacecraft [24]. The sample was taken at heliocentric distance of about 0.3 AU, far away from planet Mercury. The magnetic field components in the Radial-Tangential-Normal (RTN) reference frame are shown in the left panel of Figure 1. In this frame R indicates the radial anti-sunward direction, T is the tangential direction obtained from the cross product between the solar rotation axis and R, and N completes the frame. The time interval refers to observation made on January 14th, 2010 from 00:00:00 to 01:06:00 UT, near the mini-

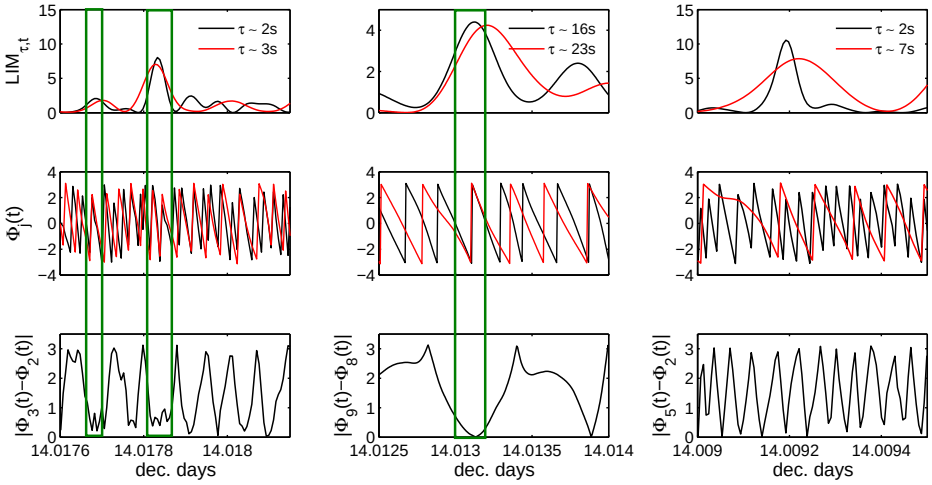

FIG. 2. Top Panels: Local Intermittency Measure (LIM) as a function of time t at two different timescales τ (see legend); middle panels: phases Φ_j of the IMFs at the τ indicated in the top panels; bottom panels: absolute value of phase difference of the two IMFs. Notation: the subscript j indicates the number of the mode, for example, $\Phi_9(t)$ is the mode number 9 having a typical timescale $\tau \sim 23$s.

mum of solar cycle 23. The magnetic field magnitude (black line) is rather steady, while the tangential (blue line) and normal (green line) components fluctuate around zero. Notice that the large scale mean magnetic field (the Parker spiral) is roughly radial near 0.3 AU. Therefore, the magnetic field variance is larger in the plane perpendicular to the mean field, indicating the presence of Alfvénic fluctuations [2]. The right panel of Figure 1 shows the Power Spectral Density (PSD) of the tangential component of **B**. The best power law fits are also indicated, both in the inertial range (thick red line) and in the high frequency range (thick blue line), with a break at $f_{br} \sim 0.2$ Hz [25, 26]. It is important to remark that the spectrum in frequency corresponds to the spectrum in the k vector space assuming that Taylor hypothesis applies [27]. High amplitude magnetic field fluctuations, described by a Kolmogorov-like energy spectrum, confirm that the sample is turbulent.

EMD of the tangential magnetic field component B_T gives $n = 18$ significant modes. In order to estimate the typical timescales, for each IMF the PSD [15] was computed (i.e., right panel of Figure 1). The modes display power either in the high frequency range (from ~ 0.2 Hz to 0.45 Hz) or in the inertial range (from 0.01 Hz to 0.1 Hz). The position in frequency,

f_i, of the peak of the PSDs of the modes (see thin red, thin blue, green, magenta, thin black, and red dashed lines in the right panel of Figure 1) gives an estimate of the characteristic time scale of each mode, $\tau_i = 1/f_i$. Therefore, IMFs with f_i above the spectral break of B_T "track" the small scale fluctuations of the field [15]. Going to lower frequencies, the large scale fluctuations of the B_T time series show up in the IMFs (not shown). Three pairs of phases of IMFs (Φ_i, Φ_j) associated with neighboring time scales are plotted in Figure 2, along with the absolute value of their phase difference $\Delta\phi \equiv \Phi_i - \Phi_j$. Left panels of Figure 2 refer to a pair of next-nearest timescales in the high frequency range of the magnetic field spectrum, middle panels to a pair of adjacent timescales within the inertial range, and right panels to one scale τ_i in the inertial range and the other scale τ_j in the high frequency range. Application of LIM to B_T provides the location of the peaks of power in the time series. We then locate the occurrence of simultaneous LIM peaks in the chosen pairs of timescales (τ_i, τ_j), as shown in top panels of Figure 2, indicating an energy transfer between the two scales.

In the left and middle columns of Figure 2, simultaneous LIM peaks (top row) are found when the two modes phases overlap (middle row), the phase difference becoming negligible (bottom row). This has been highlighted in Figure 2 through green frames. Thus, in the locations where energy is being transferred between two scales, as evidenced through simultaneous LIM peaks, phase synchronization between the modes of the field fluctuations occurs. On the contrary, phase synchronization is not correlated to LIM peaks for pairs of well separated time scales (right column of Figure 2), in agreement with a local nonlinear energy cascade. It is important to point out that phase synchronization is observed regardless of the LIM peaks amplitude (see the first frame in the left panels of Figure 2). In the framework of the multifractal energy cascade, this suggests that small intensity structures, showing phase synchronization, are also generated in the flow. Similar results hold for B_R and B_N components (not shown).

To quantitatively confirm the observation of phase synchronization, we look for statistical correlations between the phase difference of each pair of modes $(\mathrm{IMF_i}, \mathrm{IMF_j})$ and the LIM covariance at the same time scales, defined as:

$$\mathrm{Covar}(\mathrm{LIM_i}, \mathrm{LIM_j}) = \mathrm{LIM_i(t)} * \mathrm{LIM_j(t)}. \tag{3}$$

In Figure 3 we plot, for the three examples given above, the rate of occurrence of binned

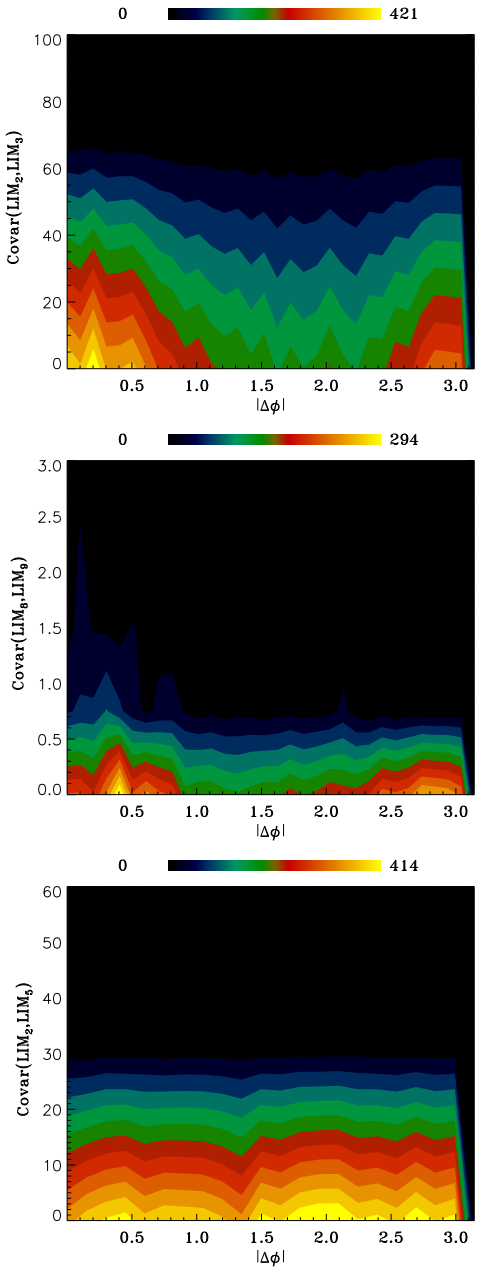

FIG. 3. 2D histograms ($|\Delta\phi|$, Covar($\mathrm{LIM_i}, \mathrm{LIM_j}$)) for the three cases displayed in Figure 2. Colors refer to the number of events stored in each bidimensional bin.

pairs ($|\Delta\phi|$, Covar($\mathrm{LIM_i}, \mathrm{LIM_j}$)). For the two cases with next-nearest modes, ($\mathrm{IMF_2}, \mathrm{IMF_3}$) and ($\mathrm{IMF_8}, \mathrm{IMF_9}$) in the high frequency and in the inertial ranges respectively, the majority of pairs have phase synchronization (small $|\Delta\phi|$), with a secondary peak at $\sim \pi$, indicating phase anticorrelation. On the contrary, the histogram for the pair ($\mathrm{IMF_2}, \mathrm{IMF_5}$), referring to separated time scales, is broad in $|\Delta\phi|$, indicating absence of correlation between phase

difference and LIM coupled peaks.

The analysis of solar wind magnetic turbulence in the inner heliosphere through coupled EMD and wavelet analyses evidences that modes of the signal on neighboring time scales have phase synchronization whenever localized peaks of magnetic energy transfer occur, regardless of their amplitude. This allows the identification of magnetic eddies generated by the turbulent cascade at different scales, and characterized by phase synchronization.

In order to test our results, the same EMD/LIM analyses has also been applied to two synthetic data sets. The first data set is a Gaussian, self-similar Wiener process [28], with no intermittent structures. The second set is an intermittent field generated through simple superposition of a Gaussian background and coherent structures sharing the same statistical properties of solar wind magnetic fluctations (see [29] for details). In this sample, intermittency is not the result of a cascade, but is simply built to mimic the statistical features of an intermittent field. Phase synchronization is not observed to be correlated to the LIM peaks in neither of the data sets (see supplemental material, Fig.s 1s, 2s for the Gaussian background+coherent structures model and Fig. 3s for the Wiener process). This confirms that phase synchronization observed in solar wind data is entirely due to the nonlinear energy turbulent cascade, which is not present in the synthetic data.

The detection and analysis of large amplitude structures in turbulent flows is usually based upon arbitrary intensity threshold techniques [9, 22, 30], able to eliminate intermittency and multifractality from the time series. These methods capture the extreme events, contained in the tails of the Probability Distribution Functions (PDFs) of fluctuations, which dominate higher order statistics. Our analysis shows that phase synchronization is observed during the occurrence of bursts of magnetic energy of any amplitude, i.e. for the whole PDF, giving information on the nonlinear energy transfer through the scales.

The results shown here indicate presence of significant phase synchronization only for comparable time scales. This is consistent with the classical picture of the local turbulent energy cascade, where nonlinear interactions mostly occur between next-nearest wave vectors [1].

Finally, phase correlation between adjacent modes is found both in the MHD inertial range and in the high frequency range of solar wind magnetic turbulence. This confirms that a nonlinear turbulent cascade is active well beyond the high frequency break (i.e. at proton scales) of the solar wind magnetic field power spectrum [14, 31], whose nature is still

matter of debate.

This work was partially supported by the Italian Space Agency, contract ASI no. I/015/07/0 "Esplorazione del Sistema Solare". SP and AV's research is supported by "Borsa Post-doc POR Calabria FSE 2007/2013 Asse IV Capitale Umano - Obiettivo Operativo M.2". SP, VC, RB, and LSV acknowledge their participation to the ISSI team 185 "Dispersive cascade and dissipation in collisionless space plasma turbulence-observations and simulations". SP, VC and LSV acknowledge the Marie Curie Project FP7 PIRSES-2010-269297 - "Turboplasmas". The authors further acknowledge the NASA Planetary Data System (PDS) for the use of the MESSENGER data.

---

[1] U. Frisch, *Turbulence: The legacy of A.N. Kolmogorov* (Cambridge University Press, Cambridge, UK, 1995).

[2] R. Bruno, and V. Carbone, Liv. Rev. Sol. Phys. **2**, 4 (2005).

[3] A.-N. Kolmogorov, Dokl. Akad. Nauk SSSR **30**, 301 (1941).

[4] L.-F. Richardson, *Weather prediction by numerical process*, Cambridge University Press (1922).

[5] E.-A. Novikov, Sov. Phys. Dokl. **14**, 104 (1969).

[6] G.-K. Batchelor, and A.-A. Townsend, in *Proceedings of the Royal Society of London. Series A, Mathematical and Physical Sciences*, **199**, 238 (The Royal Society, London, UK, 1949).

[7] G. Parisi, and U. Frisch, in *Proceedings of International School of Physics "E. Fermi"*, ed. M. Ghil, R. Benzi, and G. Parisi, 84, (North-Holland, Amsterdam, 1983).

[8] V. Carbone, P. Veltri, and R. Bruno, Phys. Rev. Lett. **75**, 3110 (1995).

[9] P. Veltri, and A. Mangeney, in *Solar Wind Nine*, ed. S.-R. Habbal, J.-V. Hollweg, and P.-A. Isenberg, **471**, 543 (American Institute of Physics, Melville, USA, 1999).

[10] A.Y.-S. Kuo, and S. Corrsin, J. Fluid Mech. **50**, 285 (1971).

[11] R. Bruno, V. Carbone, P. Veltri, E. Pietropaolo, and B. Bavassano, Plan. Space Sci. **49**, 1201 (2001).

[12] L. Sorriso-Valvo, et al., Phys. Rev. Lett. **99**, 115001 (2007).

[13] R.-J. Leamon et al., J. Geophys. Res. **103**, 4775 (1998).

[14] O. Alexandrova, V. Carbone, P. Veltri, and L. Sorriso-Valvo, Astrophys. J. **674**, 1153 (2008).

[15] N.-E. Huang et al., Proc. Math. Phys. Eng. Sci. **454**, 903 (1998).

[16] M. Farge, M. Holschneider, and J.-F. Colonna, in *Topological Fluid Mechanics*, ed. H.-K. Moffat, Cambridge University Press, 765 (1990).

[17] F. Foucher, and P. Ravier, Exp. Fluids **49**, 379 (2010).

[18] D.-A.-T. Cummings et al., Nature **427**, 344 (2004).

[19] A. Vecchio, M. Laurenza, V. Carbone, and M. Storini, Astrophys. J. Lett. **709**, L1 (2010).

[20] M. Onofri, A. Vecchio, G. De Masi, and P. Veltri, Astrophys. J. **746**, 58 (2012).

[21] A. Vecchio, M. Laurenza, D. Meduri, V. Carbone, and M. Storini, Astrophys. J. **749**, 27 (2012).

[22] M. Onorato, R. Camussi, and G. Luso, Phys. Rev E **61**, 1447 (2000).

[23] R. Bruno et al., Proc. 9th European Meeting on Solar Physics, 'Magnetic Fields and Solar Processes', ESA SP-448, Florence, Italy (1999).

[24] B.J. Anderson, et al., Space Sci. Rev. **131**, 417 (2007).

[25] S. Perri, V. Carbone, and P. Veltri, Astrophys. J. Lett. **725**, 52 (2010).

[26] H. Korth et al., Planet. Space Sci. **59**, 2075 (2011).

[27] G.-I. Taylor, Proc. R. Soc. A, **164**, 476 (1938).

[28] C.-W. Gardiner, Handbook of stochastic methods, Springer (1997).

[29] Bruno R. et al., Ann. Geophys. **22**, 3751 (2004).

[30] C. Salem, A. Mangeney, S.-D. Bale, and P. Veltri, Astrophys. J. **702**, 537 (2009).

[31] F. Sahraoui et al., Phys. Rev. Lett. **102**, 231102 (2009).